Impact of USA Oil and Natural Gas Emission Increases on Surface Ozone is most pronounced in the Central U.S.

Andrea Pozzer[1,*], Martin G. Schultz[2], and Detlev Helmig[3,a]

[1]Max Planck Institute for Chemistry, Hahn-Meitner-Weg 1, 55128 Mainz, Germany
[2]Jülich Supercomputing Centre, Forschungszentrum Jülich GmbH, Wilhelm-Johnen-Str., 52425 Jülich, Germany
[3] Boulder A.I.R. LLC, Boulder, Colorado 80305, United States
[a] now at: Boulder A.I.R. LLC, Boulder, Colorado 80303, United States
*Corresponding author: andrea.pozzer@mpic.de

Supporting Information

April 20, 2020

Number of Pages: 14

Number of Figures: 8

Number of Tables: 2

SI_Table 1. List of sites, sorted by latitude, within the NOAA Global Greenhouse Gases Reference Network (GGGRN) that provided VOC data that were used for deriving ethane global inventory estimate adjustments.

Site Code	Name	Country	Lat	Long
ALT	Alert, Nunavut	Canada	82.5	-62.5
ZEP	Ny-Alesund, Svalbard	Norway/Sweden	78.9	11.9
SUM	Summit	Greenland	72.6	-38.5
TIK	Tiksi	Russia	71.6	128.9
BRW	Barrow, Alaska	United States	71.3	-156.6
PAL	Pallas-Sammaltunturi	Finland	68.0	24.1
ICE	Storhofdi, Vestmannaeyjar	Iceland	63.3	-20.3
BAL	Baltic Sea	Poland	55.4	17.2
CBA	Cold Bay, Alaska	United States	55.2	-162.7
LLB	Lac La Biche, Alberta	Canada	55.0	-112.5
MHD	Mace Head, County Galway	Ireland	53.3	-9.9
SHM	Shemya Island, Alaska	United States	52.7	174.1
OXK	Ochsenkopf	Germany	50.0	11.8
HPB	Hohenpeissenberg	Germany	47.8	11.0
LEF	Park Falls, Wisconsin	United States	45.9	-90.3
AMT	Argyle, Maine	United States	45.0	-68.7
BSC	Black Sea, Constanta	Romania	44.2	28.7
THD	Trinidad Head, California	United States	41.1	-124.2
UTA	Wendover, Utah	United States	39.9	-113.7
AZR	Terceira Island, Azores	Portugal	38.8	-27.4
SGP	Southern Great Plains, Oklahoma	United States	36.8	-97.5
TAP	Tae-ahn Peninsula	Korea	36.7	126.1
BMW	Tudor Hill	Bermuda	32.3	-64.9
IZO	Tenerife, Canary Islands	Spain	28.3	-16.5
MID	Sand Island, Midway	United States	28.2	-177.4
KEY	Key Biscayne, Florida	United States	25.7	-80.2
ASK	Assekrem	Algeria	23.2	5.4
KUM	Cape Kumakahi, Hawaii	United States	19.5	-154.8
MLO	Mauna Loa, Hawaii	United States	19.5	-155.6
MEX	High Alt. Global Climate Obs. Ctr.	Mexico	19.0	-97.3
GMI	Mariana Islands	Guam	13.4	144.8
MKN	Mount Kenya	Kenya	-0.1	37.3
BKT	Bukit Kototabang	Indonesia	-0.2	100.3
SEY	Mahe Island	Seychelles	-4.7	55.2
NAT	Maxaranguape	Brazil	-5.5	-35.3
ASC	Ascension Island	United Kingdom	-7.9	-14.4
SMO	Tutulia	American Samoa	-14.2	-170.6
EIC	Easter Island	Chile	-27.2	-109.5
CGO	Cape Grim, Tasmania	Australia	-40.7	144.7
CRZ	Crozet Island	France	-46.5	51.9
USH	Tierra Del Fuego, Ushuaia	Argentina	-54.9	-68.5
PSA	Palmer Station	Antartica	-64.9	-64.0
SYO	Syowa Station	Antartica	-69.0	39.6
HBA	Hailey Station	UK	-75.6	-26.2
SPO	South Pole	Antartica	-90.0	-24.8

SI_Table 2. Growth rate of atmospheric ethane from Fourier-transform infrared spectroscopy (FTIR) tropospheric column measurements.

Study	Site	Site Latitude	Time Period	Rate of Change
		°N		% yr^{-1}
Hausmann et al., 2014	Zugspitze	47.4	2007-2014	3.2
Franco et al., 2015	Jungfraujoch	46.5	2009-2014	4.90 ± 0.91
Franco et al., 2016	Eureka	80	2009-2014	3.5
	Thule	77.5	2009-2014	3.2
	Jungfraujoch	46.5	2009-2014	4.9
	Toronto	43.7	2009-2014	5.4
	Boulder	40	2009-2014	5.1
	Mauna Loa	19.5	2009-2014	3.0
Helmig et al., 2016	Jungfraujoch[a]	46.5	2009.5-2015.5	4.2 ± 1.0
	Jungfraujoch[b]	46.5	2009.5-2015.5	6.0 ± 1.1
			mean:	4.3
			median:	4.6
[a]mid-troposphere				
[b]upper troposphere/lower stratosphere				

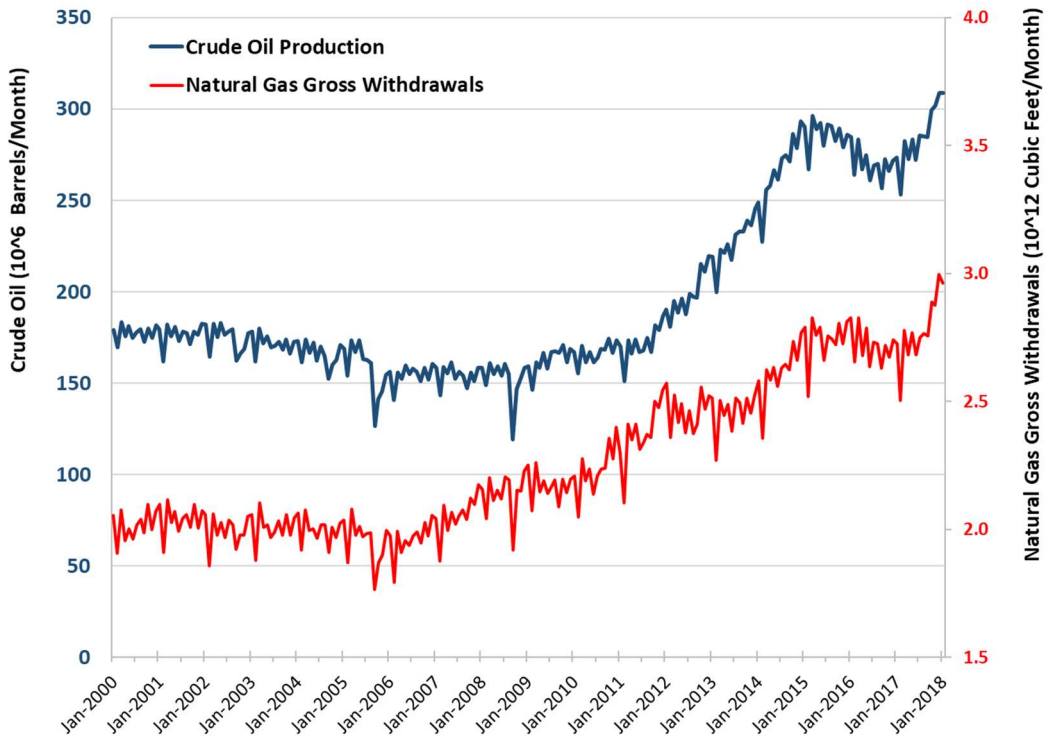

SI_Figure 1: Oil and natural gas production trends in the U.S. Oil data are from https://www.eia.gov/dnav/pet/pet_crd_crpdn_adc_mbbl_m.htm; natural gas data are from https://www.eia.gov/dnav/ng/hist/n9010us2m.htm.

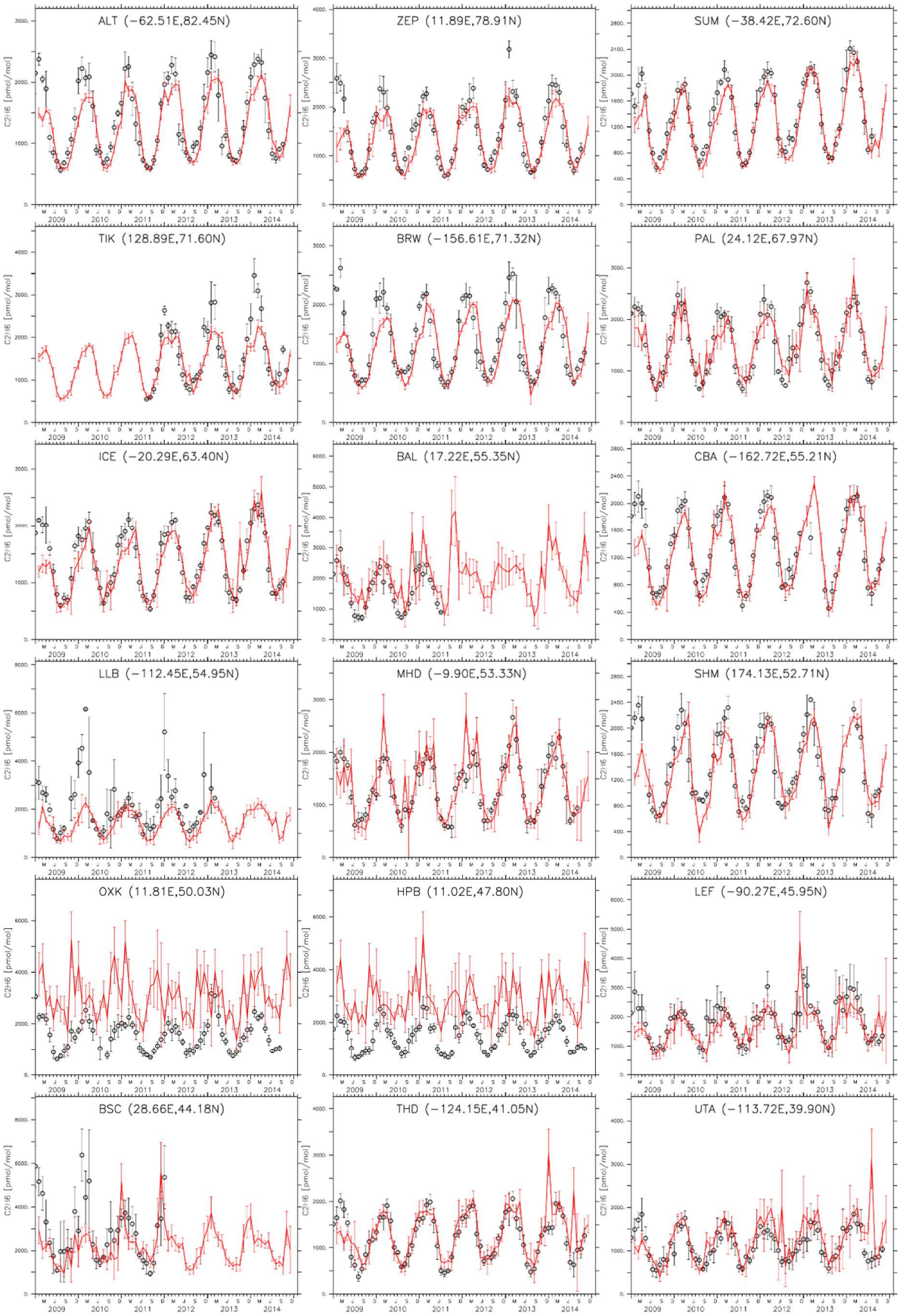

SI_Figure 2: Comparison of Global Greenhouse Gas Reference Network observations (circles) with the *Model_Run_O&NG_Trend* simulation results (red line). Monthly mean data are shown for the observations, with error bars indicating the 1-σ variability of monthly data (both for model and observations). Please see SI_Table 1 for site names and locations corresponding to the three-letter code. Graphs are arranged in order of decreasing site latitude.

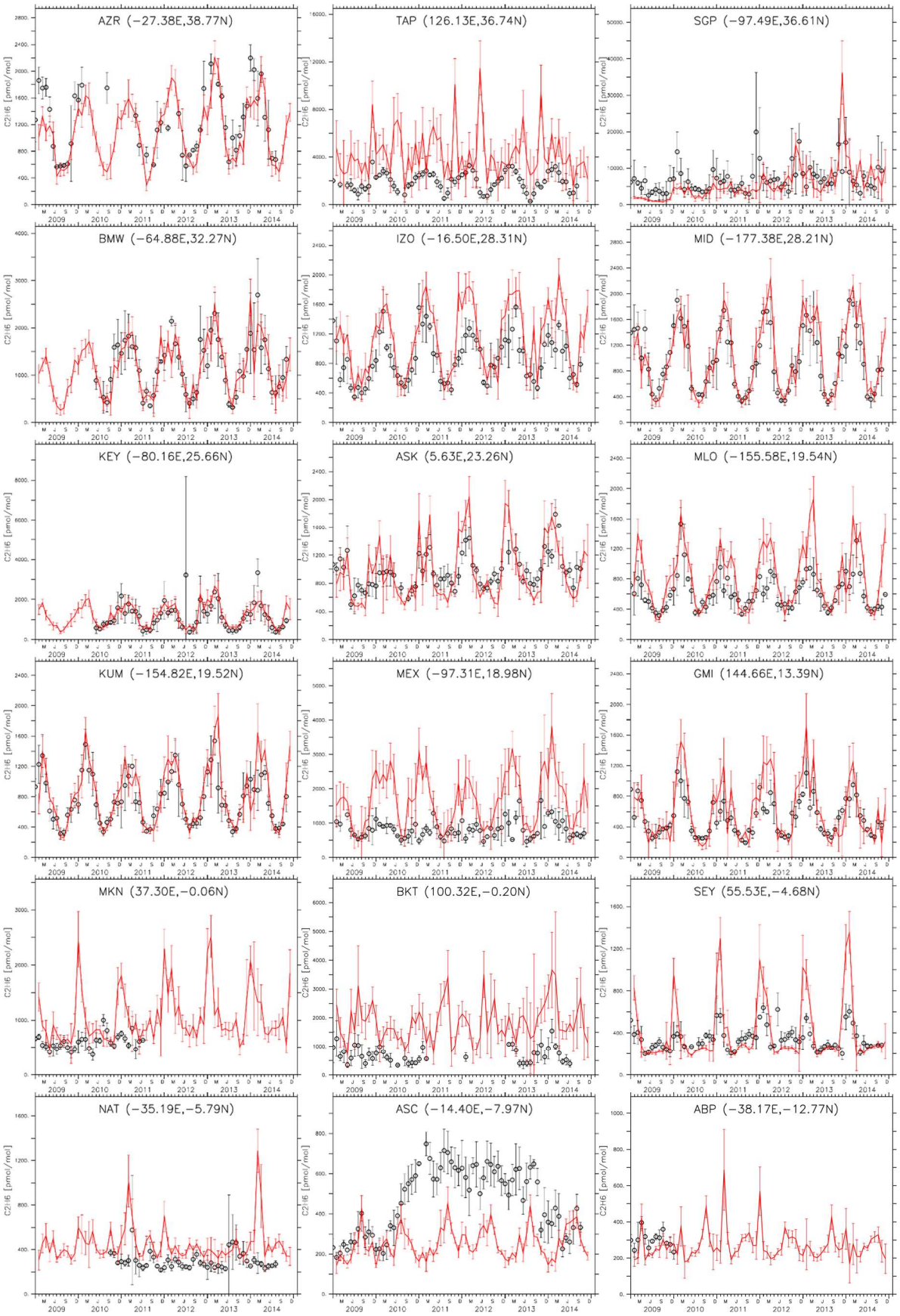

SI_Figure 2 (continued)

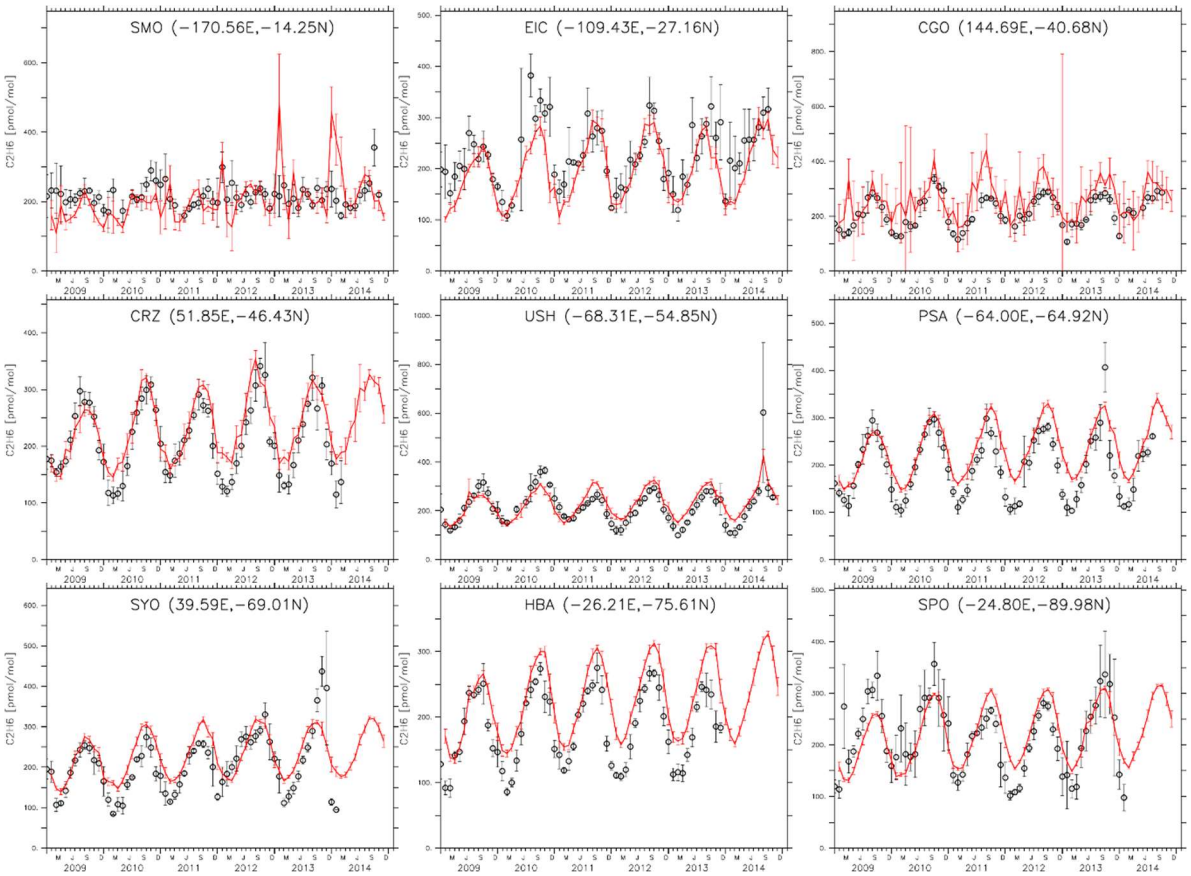

SI_Figure 2 (continued)

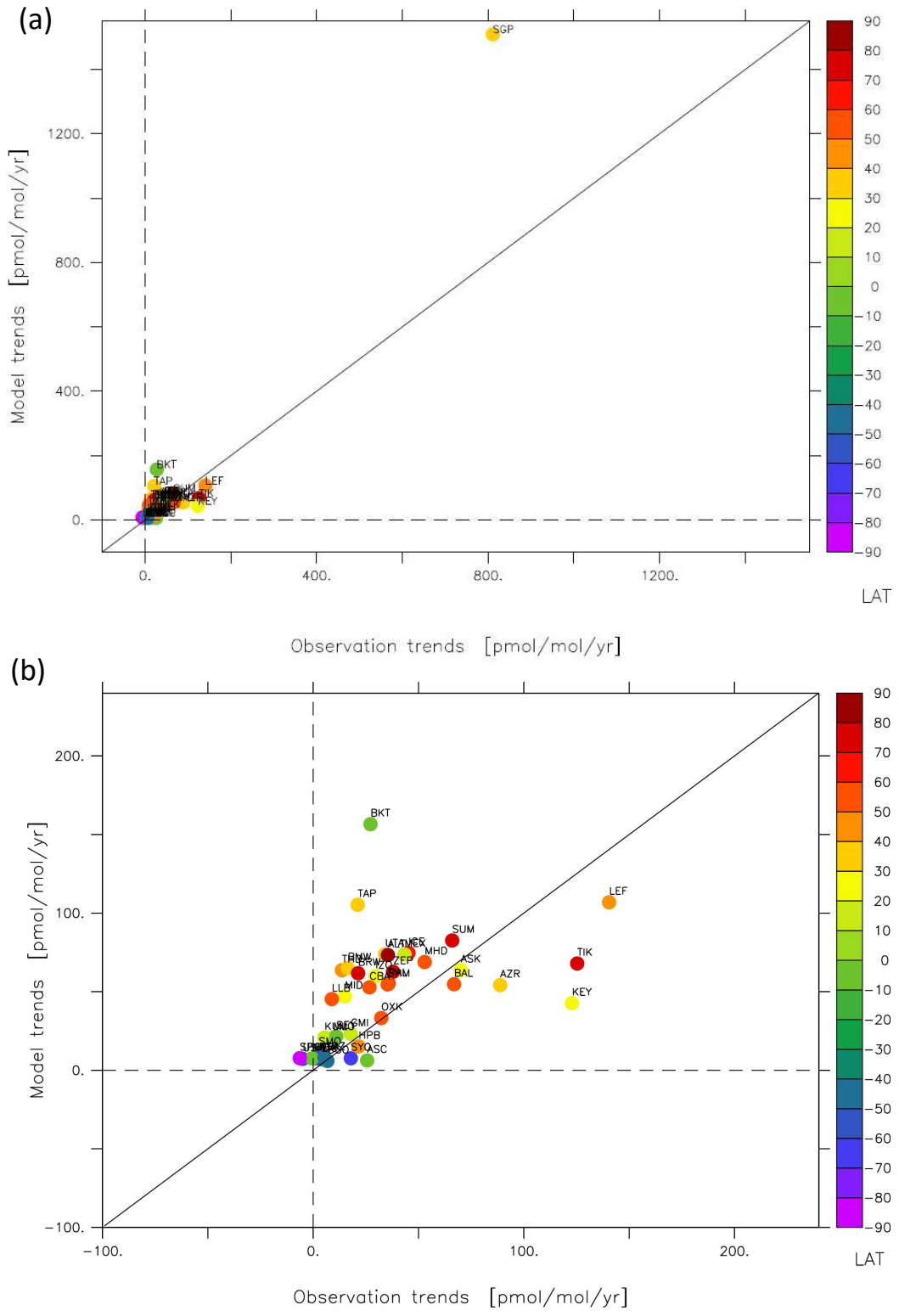

SI_Figure 3: Comparison of ethane trends seen in the observations with the *Model_Run_O&NG_Trend* model output. Data points are color coded by the site latitude according to the scale provided to the right, and labeled by the three-letter site code (SM_Table 2). (a) All data; (b) enlargement of the 0-200 pmol/mol/yr chart area.

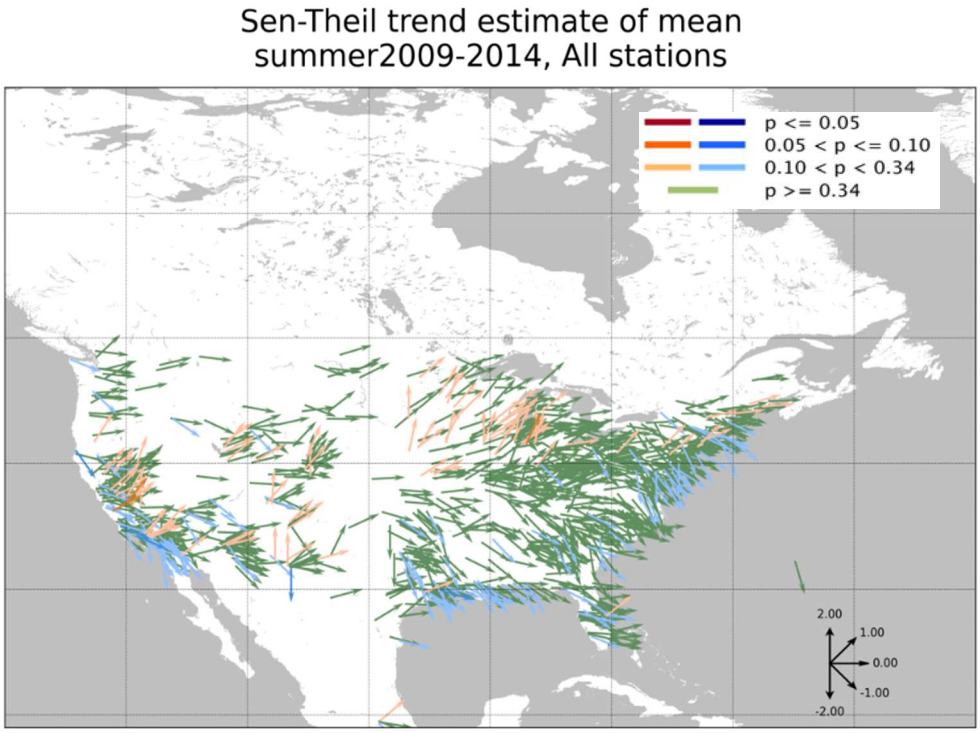

SI_Figure 4: Year 2009-2014 surface ozone trends at sites included in the Tropospheric Ozone Assessment Report (TOAR)[1]. The arrow slopes corresponds to the trend magnitude, according to the scale in the lower right of the graph, and arrow colors indicate the p-values of a Sen-Theil test of the significance of the trend slope results, as indicated in the legend.

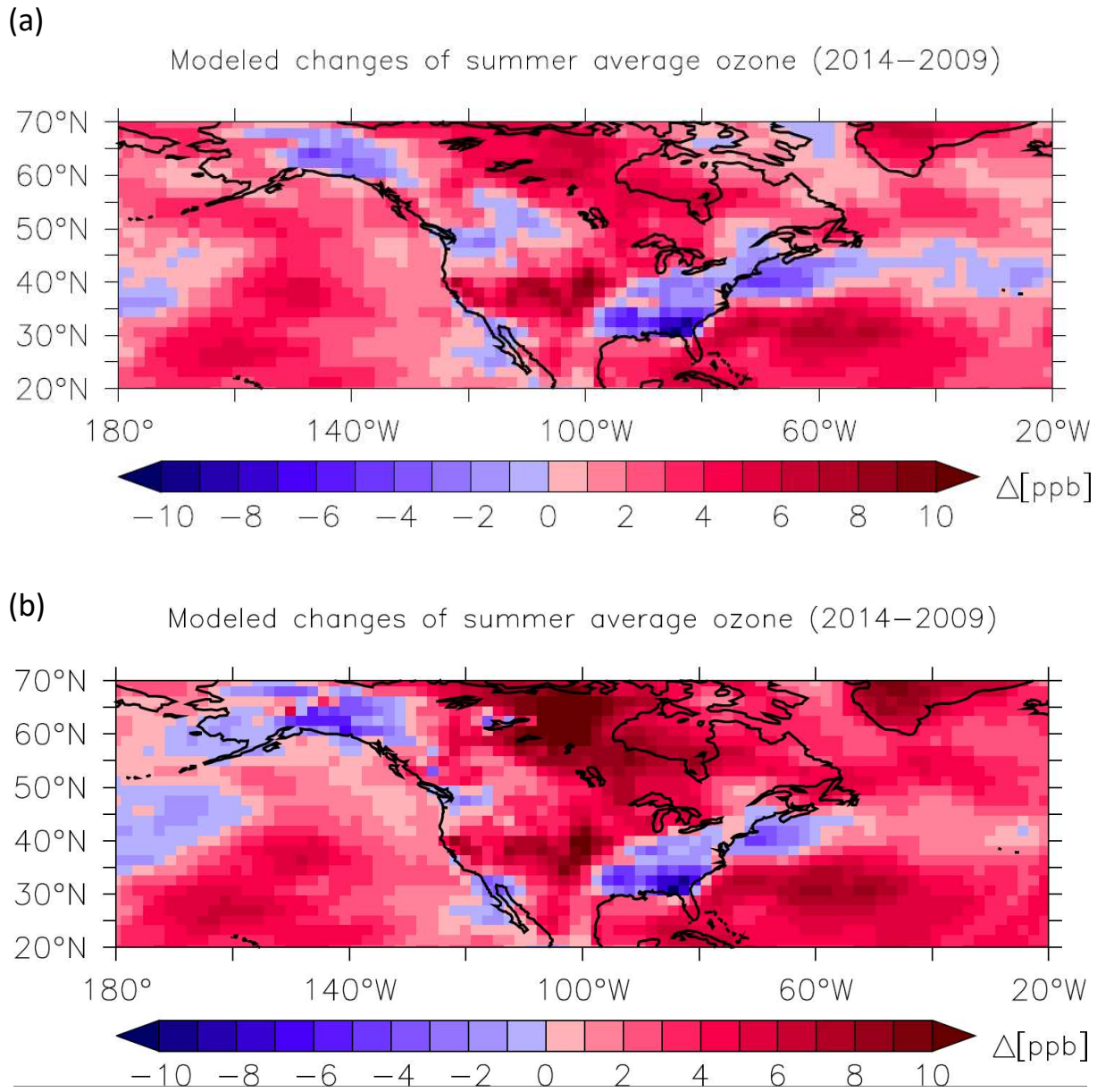

SI_Figure 5: (a) 2009 to 2014 mean summer ozone changes for North America and bordering oceans from the model run *Model_Run_Constant*, where emissions where frozen to 2009 levels. Ozone changes in this analysis primarily reflect meteorological influences over this time window. (b) Results from the *Model_Run_O&NG_Trend.*

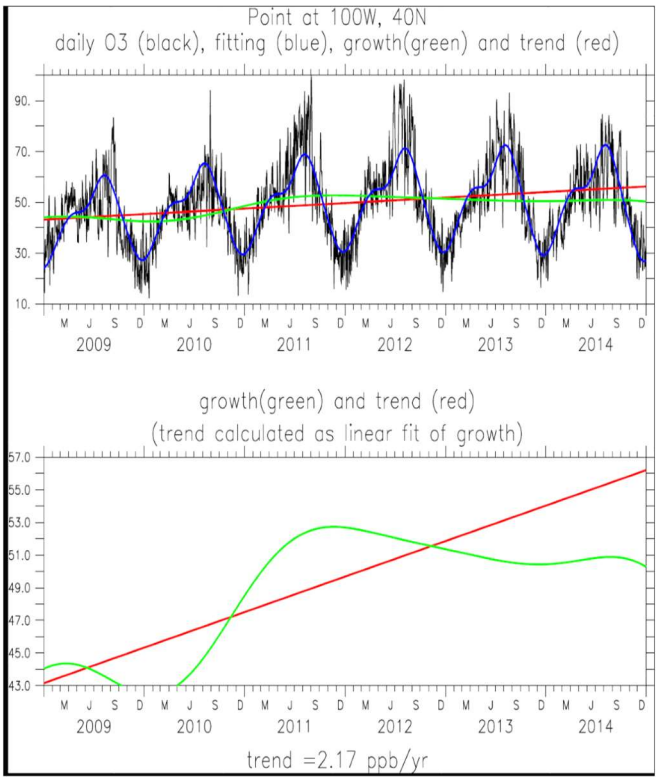

SI_Figure 6: Ozone output from the model for a midwestern U.S. location (100°W, 40°N) (*Model_Run_O&NG_Trend*) with fitting results for year-to-year changes (green) and linear trend (red) fit through the 2009-2014 data.

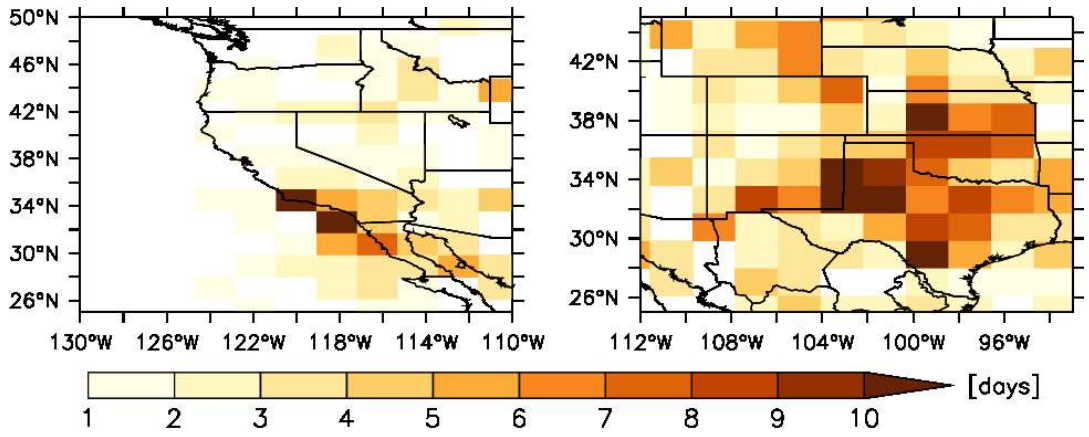

SI_Figure 7: Enlargements of results shown in Figure 3 of the main paper, showing additional days with 8-hour ozone >70 ppb for the Central US and California from the O&NG emissions growth from 2009 to 2014.

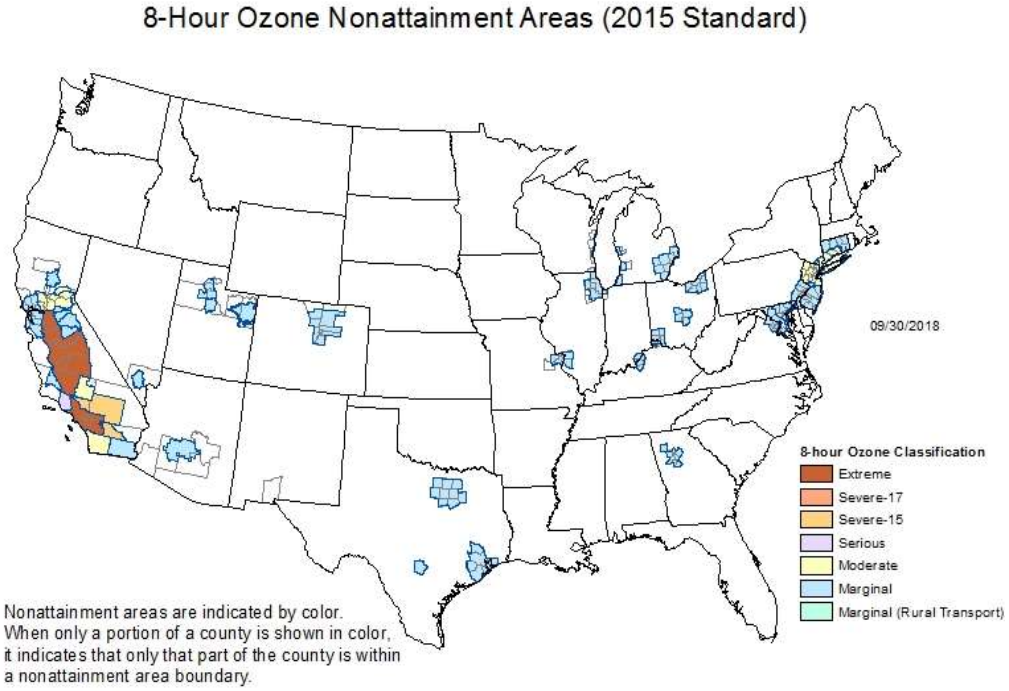

SI_Figure 8: U.S. map showing counties that as of September 2018 were in non-attainment of the 2015 ozone NAAQS (https://www3.epa.gov/airquality/greenbook/map8hr_2015.html).

SI_Text 1

Following a reviewer's suggestion, we conducted a preliminary assessment of the health effects from the oil and gas – produced ozone. We estimated mortality associated with long exposure to elevated ozone levels, which is linked to increased chronic obstructive pulmonary disease (COPD). The model was based on the exposure-response function from [2], using updated coefficient, as presented by [3], and followed the methodology described in [4] and [5]. The population data for the USA were from the NASA Socioeconomic Data and Applications Center (SEDAC), hosted by the Columbia University Center for International Earth Science Information Network (CIESIN), available at a resolution of 2.5′ × 2.5′ (about 5 km × 5 km) (http://sedac.ciesin.columbia.edu/). The total U.S. COPD mortality was obtained from the Global Burden of Disease (GBD) database for the year 2014 (http://www.healthdata.org/gbd). Based on these input data and modeling, we estimated that on average approximately 12308 (11208-13208 with a CL of 95%) people died prematurely in 2014 due to ozone pollution. This number is reduced to 12099 (10977-13021 with a CL of 95%) in a model run that excludes the added oil and gas emissions and the additional ozone formed from these emissions. Consequently, this calculation estimates that the ozone that is produced from the added oil and gas emissions is responsible for an additional ~320 premature deaths per year. This number is lower than the 970 (range 520-1400) premature deaths from the total oil and gas-produced ozone that were projected for 2025 for the U.S. by Fann et al. [2018]. At least part of this difference can likely be explained by the time difference of these studies, i.e. the 11 years of continued growth of the O&NG industry and associated emissions that were considered by Fann et al. [2018]. Further, our estimate has a relatively high uncertainty for numerous reasons, including the coarse resolution of the ECHAM model. There will be areas within

each grid where the produced ozone is higher than the value calculated for the grid cell on average, and there will be areas where ozone will be lower. Given the non-linearity of the mortality-ozone relationship, it is more likely that our estimate is an underestimate rather than a high estimate. Please also note that this mortality estimate does not include possible reductions in mortality from the decreased emissions that result from the transition of coal to natural gas powered electricity generating plants.

Supporting Information References

1. Schultz, M. G.; Schroder, S.; Lyapina, O.; Cooper, O. R.; Galbally, I.; Petropavlovskikh, I.; von Schneidemesser, E.; Tanimoto, H.; Elshorbany, Y.; Naja, M.; Seguel, R. J.; Dauert, U.; Eckhardt, P.; Feigenspan, S.; Fiebig, M.; Hjellbrekke, A. G.; Hong, Y. D.; Kjeld, P. C.; Koide, H.; Lear, G.; Tarasick, D.; Ueno, M.; Wallasch, M.; Baumgardner, D.; Chuang, M. T.; Gillett, R.; Lee, M.; Molloy, S.; Moolla, R.; Wang, T.; Sharps, K.; Adame, J. A.; Ancellet, G.; Apadula, F.; Artaxo, P.; Barlasina, M. E.; Bogucka, M.; Bonasoni, P.; Chang, L.; Colomb, A.; Cuevas-Agullo, E.; Cupeiro, M.; Degorska, A.; Ding, A. J.; FrHlich, M.; Frolova, M.; Gadhavi, H.; Gheusi, F.; Gilge, S.; Gonzalez, M. Y.; Gros, V.; Hamad, S. H.; Helmig, D.; Henriques, D.; Hermansen, O.; Holla, R.; Hueber, J.; Im, U.; Jaffe, D. A.; Komala, N.; Kubistin, D.; Lam, K. S.; Laurila, T.; Lee, H.; Levy, I.; Mazzoleni, C.; Mazzoleni, L. R.; McClure-Begley, A.; Mohamad, M.; Murovec, M.; Navarro-Comas, M.; Nicodim, F.; Parrish, D.; Read, K. A.; Reid, N.; Ries, N. R. L.; Saxena, P.; Schwab, J. J.; Scorgie, Y.; Senik, I.; Simmonds, P.; Sinha, V.; Skorokhod, A. I.; Spain, G.; Spangl, W.; Spoor, R.; Springston, S. R.; Steer, K.; Steinbacher, M.; Suharguniyawan, E.; Torre, P.; Trickl, T.; Lin, W. L.; Weller, R.; Xu, X. B.; Xue, L. K.; Ma, Z. Q., Tropospheric Ozone Assessment Report: Database and metrics data of global surface ozone observations. *Elementa-Science of the Anthropocene* **2017,** *5*, 1-23.
2. Ostro, B., Outdoor Air Pollution: Assessing the Environmental Burden of Disease at National and Local Levels. *World Health Organization Environmental Burden of Disease Series* **2004,** *No. 5*, (Geneva).
3. Cohen, A. J.; Brauer, M.; Burnett, R.; Anderson, H. R.; Frostad, J.; Estep, K.; Balakrishnan, K.; Brunekreef, B.; Dandona, L.; Dandona, R.; Feigin, V.; Freedman, G.; Hubbell, B.; Jobling, A.; Kan, H.; Knibbs, L.; Liu, Y.; Martin, R.; Morawska, L.; Pope, C. A.; Shin, H.; Straif, K.; Shaddick, G.; Thomas, M.; van Dingenen, R.; van Donkelaar, A.; Vos, T.; Murray, C. J. L.; Forouzanfar, M. H., Estimates and 25-year trends of the global burden of disease attributable to ambient air pollution: an analysis of data from the Global Burden of Diseases Study 2015. *Lancet* **2017,** *389*, (10082), 1907-1918.
4. Jerrett, M.; Burnett, R. T.; Pope, C. A.; Ito, K.; Thurston, G.; Krewski, D.; Shi, Y. L.; Calle, E.; Thun, M., Long-term ozone exposure and mortality. *New England Journal of Medicine* **2009,** *360*, (11), 1085-1095.
5. Lelieveld, J.; Evans, J. S.; Fnais, M.; Giannadaki, D.; Pozzer, A., The contribution of outdoor air pollution sources to premature mortality on a global scale. *Nature* **2015,** *525*, (7569), 367-371.